Emergence and bifurcations of Lyapunov manifolds in nonlinear wave equations

Taoufik Bakri*, Hil G.E. Meijer†and Ferdinand Verhulst

Mathematisch Instituut

University of Utrecht

PO Box 80.010, 3508 TA Utrecht

The Netherlands

March 12, 2009

Abstract

Persistence and bifurcations of Lyapunov manifolds can be studied by a combination of averaging-normalization and numerical bifurcation methods. This can be extended to infinite-dimensional cases when using suitable averaging theorems. The theory is applied to the case of a parametrically excited wave equation. We find fast dynamics in a finite, resonant part of the spectrum and slow dynamics elsewhere. The resonant part corresponds with an almost-invariant manifold and displays bifurcations into a wide variety of phenomena among which are 2- and 3-tori.

Corresponding author: Ferdinand Verhulst

*now at TNO Built Environment and Geosciences, P.O. Box 49, 2600 AA Delft, The Netherlands

†now at Twente University, PO Box 217, 7500 AE Enschede, The Netherlands

Key words: nonlinear waves, averaging, bifurcations, resonance, parametric excitation.

AMS Classification: 35L70, 35B32, 37G15, 74J30.

1 Introduction

The periodic solutions, found in linear ODEs and linear evolution equations (PDEs) play a basic role in the analysis of natural phenomena. Classical examples are the harmonic equation and the linear wave equation in one or more space dimensions. Complications in the analysis arise when coupling such equations and even more so if nonlinear terms are taken into account. A natural approach is to identify periodic solutions in the uncoupled and linearized system and to look for the changes caused by coupling and nonlinear terms by continuation and bifurcation techniques. These periodic solutions from linearized systems are located on normal mode manifolds, also called Lyapunov manifolds.

A well-known but already non-trivial example is the case of two nonlinearly coupled anharmonic equations of the form

$$\ddot{x}_i + \omega_i^2 x_i = \varepsilon f_i(x, \dot{x}),\ x = (x_1, x_2), i = 1, 2.$$

In the limit $\varepsilon = 0$, the system is decoupled and two (harmonic) one degree of freedom systems exist with solutions filling up two two-dimensional (normal mode) Lyapunov manifolds. A basic question is then whether these manifolds can be continued for small $\varepsilon > 0$. If this is the case, they will be located in a neighbourhood of the exact $\varepsilon = 0$ Lyapunov manifolds that shrinks to zero with $\varepsilon \to 0$. In a neighbourhood of the origin of phase space and as $\varepsilon \to 0$, they are tangent to the $\varepsilon = 0$ normal mode manifolds. In the case of the two coupled harmonic equations, this question was solved a long time ago.

A second basic and largely unsolved question is whether the Lyapunov manifolds persist for increasing ε and other changes of relevant parameters. Possible tools to study these questions are averaging-normalization and numerical bifurcation theory. As we will show, the combination of both techniques is very powerful. For ODEs these questions are difficult enough, but we will be especially interested in bifurcations of Lyapunov manifolds in the case of infinite dimensional systems. Extension of averaging to infinite-dimensional problems is possible and was carried out during the last decade, but it raises special difficulties, depending on the choice of operator and the type of problem formulation (parabolic or hyperbolic, infinite or bounded spatial domains); for references see section 2.

In the next section we will describe two theorems that can be used in an infinite dimensional setting. It is remarkable that these theorems are not widely known. It will be seen in the next section, that the technique of averaging-normalization produces a system, simplified by normalization. Solving the system and inverting the normalizing transformation gives the solution (without approximation) of the original problem. As we shall describe in what follows, in practice one omits higher order terms to obtain approximate solutions. Interestingly, the normalization procedure gives a short-cut to slow-fast dynamics. Removing the non-resonant terms, one finds normally hyperbolic manifolds from the normalized equations because of the dominating presence of slow-fast dynamics, and one can then ask, whether these manifolds persist in the original system. One of the two theorems, formulated for an infinite-dimensional setting, the Sanchez-Palencia theorem, allows us to conclude the validity of approximations for all time. However, we shall argue that this qualitative information is not enough to prove the existence of such manifolds in the original system. Instead we will introduce the notion of 'almost-invariant' manifold.

We demonstrate this slow-fast dynamics, produced by averaging-normalization, for a para-

metrically excited wave equation that has as an additional interest, the suggestion in [10] that this equation could not be handled by the usual and well-established perturbation techniques. Our analysis shows that perturbation analysis does not fail, but that surprisingly enough, a complicated bifurcation structure destroys this picture for relatively small values of the small parameter ε. For this part of the analysis we use higher order averaging in the case of near-resonance ([11]) and we use numerical bifurcation techniques as described in [6] and implemented in [7, 8].

For the terminology of normal forms, resonance, near-resonance etc., we refer to [11]. We stress finally that the emergence of slow-fast dynamics by averaging-normalization is a phenomenon common to many hyperbolic nonlinear PDE problems. Therefore, the phenomenon we describe, is rather general and it is caused by the presence of resonant and non-resonant terms in the original problem which obscure the underlying dynamics. An extensive discussion and a number of examples can be found in [16], section 13.3.

2 Normal forms for wave equations

Consider the semilinear initial value problem

$$\frac{dw}{dt} + \mathcal{A}w = \varepsilon f(w, t, \varepsilon), \quad w(0) = w_0, \tag{1}$$

where $-\mathcal{A}$ generates a uniformly bounded C_0-group $G(t), -\infty < t < +\infty$, on the Banach space X.

We assume the following *basic conditions*:

- f is continuously differentiable and uniformly bounded on $\bar{D} \times [0, \infty) \times [0, \varepsilon_0]$, where D is an open, bounded set in X.

- f can be expanded with respect to ε in a Taylor series, at least to some order.

2.1 Integral equation and standard form

A generalized solution of Eq. (1) is defined as a solution of the integral equation:

$$w(t) = G(t)w_0 + \varepsilon \int_0^t G(t-s)f(w(s), s, \varepsilon)ds.$$

It is well-known that under the given conditions for f and with the uniform boundedness of $G(t)$ the integral equation has a unique solution that exists on the timescale $1/\varepsilon$. The proof follows the usual contraction construction in Banach spaces.

Using the variation of constants transformation $w(t) = G(t)z(t)$ for Eq. (1), we find the integral equation corresponding with the so-called standard form (see [11] or [16])

$$z(t) = w_0 + \varepsilon \int_0^t F(z(s), s, \varepsilon)ds, \quad F(z, s, \varepsilon) = G(-s)f(G(s)z, s, \varepsilon). \tag{2}$$

2.2 Averaging normal form

We assume that $F(z, s, \varepsilon)$ is an almost-periodic function in a Banach space, satisfying Bochner's criterion, see for instance [16]. The average F^0 is defined by:

$$F^0(z) = \lim_{T\to\infty} \frac{1}{T} \int_0^T F(z, s, 0)ds. \tag{3}$$

Applying normalization by the averaging transformation

$$z(t) = v(t) + \varepsilon \int_0^t \left(F(v, s, 0) - F^0(v)\right) ds, \ v(0) = w_0, \tag{4}$$

produces the normal form equation

$$v(t) = w_0 + \varepsilon \int_0^t F^0(v(s))ds + O(\varepsilon^2).$$

After introducing transformation (4), we can still obtain the exact solution by solving the resulting equation for $v(t)$ including the $O(\varepsilon^2)$-terms, to find $z(t)$ from (4) and then $w(t)$. The averaging approximation $\bar{z}(t)$ of $z(t)$ is obtained by omitting the $O(\varepsilon^2)$-terms:

$$\bar{z}(t) = w_0 + \varepsilon \int_0^t F^0(\bar{z}(s))ds, \tag{5}$$

or alternatively

$$\frac{d\bar{z}}{dt} = \varepsilon F^0(\bar{z}),\ \bar{z}(0) = w_0. \tag{6}$$

Under these rather general conditions, [4] (or [16]) provides the following theorem:

Theorem 2.1

(general averaging)

Consider Eq. (1) and the corresponding $z(t)$, $\bar{z}(t)$ given by Eqs. (2) and (5) under the basic conditions stated above. If $G(t)\bar{z}(t)$ exists in an interior subset of D on the timescale $1/\varepsilon$, we have

$$z(t) - \bar{z}(t) = o(1) \text{ as } \varepsilon \to 0$$

on the timescale $1/\varepsilon$. If $F(z, t, 0)$ is periodic in t, the error is $O(\varepsilon)$.

2.3 Application to hyperbolic equations

A straightforward application is to consider semilinear initial value problems of hyperbolic type,

$$u_{tt} + Au = \varepsilon f(u, u_t, t, \varepsilon), \quad u(0) = u_0, u_t(0) = v_0, \tag{7}$$

where A is a positive, self-adjoint linear operator on a separable Hilbert space and f satisfies the basic conditions. In our application later on, we will be concerned with the case that we have one space dimension and that for $\varepsilon = 0$ we have a linear, dispersive wave equation by

choosing:

$$Au = -u_{xx} + u.$$

To make the relation with Eq. (1) explicit, one writes $u_1 = u, u_2 = u_t$ and

$$\begin{aligned} \frac{\partial u_1}{\partial t} &= u_2, \\ \frac{\partial u_2}{\partial t} &= -Au_1 + \varepsilon f(u_1, u_2, t, \varepsilon). \end{aligned}$$

One uses the operator (with eigenvalues and eigenfunctions) associated with this system.

In particular and to focus ideas, consider the case of the boundary conditions $u(0,t) = u(\pi,t) = 0$.

In this case, a suitable domain for the eigenfunctions is $\{u \in W^{1,2}(0,\pi) : u(0) = u(\pi) = 0\}$. Here $W^{1,2}(0,\pi)$ is the Sobolev space consisting of functions $u \in L_2(0,\pi)$ that have first-order generalised derivatives in $L_2(0,\pi)$. The eigenvalues are $\lambda_n = \sqrt{n^2+1}, n = 1, 2, \cdots$ and the spectrum is nonresonant. The implication is that $F(z,s,0)$ in expression (3) is almost-periodic.

Assume now for Eq. (7) homogeneous Dirichlet conditions or homogeneous Neumann conditions. The denumerable eigenvalues in this case are $\lambda_n = \omega_n^2$ and the corresponding eigenfunctions $v_n(x)$ with $n = 1, 2, 3, \ldots$. Substitution of the expansion $\sum u_n(t)v_n(x)$ and taking inner products, produces the infinite set of coupled second-order equations

$$\ddot{u}_n + \omega_n^2 u_n = \varepsilon F(\mathbf{u}), \tag{8}$$

with $\mathbf{u}$ representing the infinite set $u_n, \dot{u}_n$ with $n = 1, 2, 3, \ldots$ in the Dirichlet case, $n = 0, 1, 2, \ldots$ in the Neumann case.

2.4 The Sanchez-Palencia theorem

In the case of attraction, averaging-normalization leads to stronger approximation results. The results can be described as follows. Consider the initial value problem in a Banach space

$$\dot{x} = \varepsilon f(x,t),\ x(0) = x_0.$$

Suppose that we can average the vector field:

$$f^0(z) = \lim_{T\to\infty} \frac{1}{T} \int_0^T f(z,s)ds$$

and thus can consider the averaged equation

$$\dot{z} = \varepsilon f^0(z),\ z(0) = x_0.$$

We have the following result:

Theorem 2.2

Suppose that the vector fields f and f^0 are continuously differentiable and that $z = a$ is an asymptotically stable critical point (in linear approximation) of the averaged equation. If x_0 lies within the domain of attraction of a, we have

$$x(t) - z(t) = o(1) \text{ as } \varepsilon \to 0$$

for $t \geq 0$. If the vector field f is periodic in t, the error is $O(\varepsilon)$ for all time.

The result is based on [12] and [13]; for more details and examples in the finite-dimensional context see [11]. Note however, that the proof in [11] immediately carries over to a Banach space, as in [13].

2.5 Slow-fast dynamics

In our analysis of the hyperbolic PDE (7), we will be interested in the case that we have a resonance between a finite number of modes k and that the infinite number of other,

non-resonant modes are attracted to a stationary solution. To fix ideas, assume that these stationary states correspond with the trivial solutions of the modes as will be the case in our example. The attraction is produced by dissipation and it is natural to include in the $O(\varepsilon)$ term of Eq. (7) the term $-\varepsilon\beta u_t$ so that $f(u, u_t, t, \varepsilon)$ is replaced by $-\beta u_t + f(u, u_t, t, \varepsilon)$ with $\beta > 0$, independent of ε.

With these assumptions, we shall split system (8) into two subsystems. First the finite-dimensional system:

$$\ddot{u}_n + \omega_n^2 u_n = -\varepsilon\beta\dot{u}_n + \varepsilon f_1(u_0, \dot{u}_0, \ldots, u_k, \dot{u}_k) + \varepsilon^2 f_2(\mathbf{u}) + \varepsilon^3 \cdots, \ n = 0, 1, \ldots, k, \tag{9}$$

where we have removed the non-resonant terms by normalization (with some abuse of notation, we keep using the variable u_n). Because of the assumption of non-resonance for the modes starting with $n = k+1$, the averaging process leaves in the second, infinite-dimensional system to first order only the dissipative term:

$$\ddot{u}_n + \omega_n^2 u_n = -\varepsilon\beta\dot{u}_n + \varepsilon^2 g_2(\mathbf{u})) + \varepsilon^3 \cdots, n = k+1, k+2, \ldots. \tag{10}$$

Omitting the $O(\varepsilon^2)$ terms in the finite-dimensional system (9), we will analyse the system

$$\ddot{u}_n + \omega_n^2 u_n = -\varepsilon\beta\dot{u}_n + \varepsilon f_1(u_0, \dot{u}_0, \ldots, u_k, \dot{u}_k), \ n = 0, 1, \ldots, k, \tag{11}$$

looking for attracting (hyperbolic) invariant sets.

The explicit averaging-normalization transformation for the second (infinite-dimensional) system (10) starts with the standard transformation $u_n, \dot{u}_n \to y_{n_1}, y_{n_2}$

$$\begin{aligned} u_n &= y_{n_1}\cos\omega_n t + \frac{y_{n_2}}{\omega_n}\sin\omega_n t, \\ \dot{u}_n &= -\omega_n y_{n_1}\sin\omega_n t + y_{n_2}\cos\omega_n t, \ n = k+1, k+2, \cdots, \end{aligned}$$

followed by averaging. Omitting the $O(\varepsilon^2)$ terms, this produces the system

$$\dot{y}_{n_1} = -\frac{1}{2}\varepsilon\beta y_{n_1}, \ \dot{y}_{n_2} = -\frac{1}{2}\varepsilon\beta y_{n_2}, \ n = k+1, k+2, \ldots.$$

The solutions decay exponentially to zero and according to the Sanchez-Palencia theorem 2.2 we have

$$\begin{aligned} u_n(t) &= e^{-\frac{1}{2}\varepsilon\beta t}(u_n(0)\cos\omega_n t + \frac{\dot{u}_n(0)}{\omega_n}\sin\omega_n t) + o(1), \\ \dot{u}_n(t) &= e^{-\frac{1}{2}\varepsilon\beta t}(-u_n(0)\omega_n\sin\omega_n t + \dot{u}_n(0)\cos\omega_n t) + o(1), \end{aligned}$$

$n = k+1, k+2, \cdots$, with the estimates $o(1)$ as $\varepsilon \to 0$ and *validity of the estimates for all positive time* ($t \geq 0$). For the energy of the modes of system (10) we have

$$E_n(t) = \frac{1}{2}(\dot{u}_n^2(t) + \omega_n^2 u_n^2(t)) = E_n(0)e^{-\varepsilon\beta t} + o(1)$$

for all time. We conclude that after an interval of time, asymptotically larger than $1/\varepsilon$ (for instance $1/\varepsilon^2$), the righthand sides of the second (infinite-dimensional) system after averaging-normalization become $o(1)$. Starting with $o(1)$ initial conditions, the non-resonant modes remain $o(1)$.

In this way we have arrived at an explicit construction of slow-fast dynamics by asymptotics. The infinite-dimensional system (10) represents after some time or with small initial values the slow dynamics, the resonant system (9) the fast one. The hyperbolic invariant sets of the resonant system are normally hyperbolic in the complete system. Note however, that we have the following issues; some of them need further discussion:

1. By higher order averaging-normalization, we can remove all resonant modes $1, \cdots, k$ from the non-resonant system (10). Using these transformations, the error estimates will improve, the solutions of system (10) are shown to approach the trivial solutions with even higher precision. In this way, we have an explicit justification of restricting our analysis to the finite-dimensional resonant system as $\varepsilon \to 0$. The manifold M spanned by the first k modes is 'almost-invariant'.

2. The asymptotic results obtained are valid as $\varepsilon \to 0$ and this poses the classical problem of what happens when increasing ε; see the discussion in [16], section 10.5. As we will show in an application in the next section, continuation of ε away from 0 in higher dimensional systems, leads to interesting bifurcations.

3. Related to the preceding item is the problem of accidental resonance. We have excluded this by our assumptions, however we did not exclude *near* accidental resonance. Again, this plays no part as $\varepsilon \to 0$, but the phenomenon comes up when increasing ε in a high-, even infinite-dimensional, system. This will also be demonstrated later on.

4. Nontrivial hyperbolic, stationary solutions of system (11) produce solutions of a particular form. The corresponding resonant modes can be written as a harmonic (periodic) function plus an $o(1)$ (probably almost-periodic) function. The non-resonant modes are $o(1)$ solutions.

5. If the manifold M, discussed in the first item, is compact, it is a serious candidate to put it in the framework of Fenichel's slow manifold theory. Extension to infinite-dimensional problems of Fenichel theory is possible but raises special difficulties, depending on the choice of operator and the type of problem formulation. A discussion on parabolic and hyperbolic problems can be found in [1], see also [2], [3], [9] and [18]. In [5] the emphasis is on the persistence of invariant manifolds in dissipative equations, the main technique is contraction which takes often the form of Gronwall's lemma.

   In this rather general framework we can not prove the existence of a slow manifold as we can not exclude small chaotic behavior at higher order. The possibility of such phenomena was also observed in [17]. Note however, that our results are stronger than formal, as the 'almost-invariance' of the manifold M has been established rigorously.

3 A parametrically excited wave equation

An interesting problem was studied by Rand et al. in [10], where they considered the wave equation

$$u_{tt} - c^2 u_{xx} + \varepsilon\beta u_t + (\omega_0^2 + \varepsilon\gamma\cos t)u = \varepsilon\alpha u^3,\ t \geq 0, 0 < x < \pi, \tag{12}$$

with boundary conditions $u_x(0,t) = u_x(\pi,t) = 0$ and $\beta > 0$ (damping). For $\varepsilon = 0$ the model reduces to the dispersive wave equation of section 2.3, also we shall see that the discussion on slow-fast dynamics of section 2.5 applies. In [10] the experimental motivation for this model is discussed, firstly a line of coupled pendula with vertical (parametric) forcing and secondly the behavior of water waves in a vertically forced channel. Related mechanical problems can be found in [14].

3.1 Modal expansion

Using the eigenfunctions $v_n(x) = \cos nx$, and eigenvalues

$$\omega_n^2 = \omega_0^2 + n^2 c^2,\ n = 0, 1, 2, \cdots, \tag{13}$$

we expand the solution as

$$u(x,t) = \sum_0^\infty u_n(t)\cos nx.$$

Taking L_2-inner products with $v_n(x)$ produces the infinite dimensional system

$$\ddot{u}_n + \omega_n^2 u_n = \varepsilon(-\beta\dot{u}_n - \gamma u_n\cos t + \alpha g_n(\mathbf{u})),\ n = 0, 1, 2, \cdots, \tag{14}$$

with $\mathbf{u} = (u_0, u_1, u_2, \cdots)$ and suitable initial conditions. The g_n are infinite, homogeneous cubic series in $u_0, u_1, u_2, \cdots$ with terms of the form

$$u_n^3, u_i^2 u_j (i \neq j), u_i u_j u_l (i \neq j \neq l).$$

For example in the case of truncating the expansion to the first three modes, we have

$$\begin{aligned} g_0 &= u_0^3 + \tfrac{3}{2}u_0u_1^2 + \tfrac{3}{2}u_0u_2^2 + \tfrac{3}{4}u_1^2u_2, \\ g_1 &= \tfrac{3}{4}u_1^3 + 3u_0^2u_1 + \tfrac{3}{2}u_1u_2^2 + 3u_0u_1u_2, \\ g_2 &= \tfrac{3}{4}u_2^3 + 3u_0^2u_2 + \tfrac{3}{2}u_1^2u_2 + \tfrac{3}{2}u_0u_1^2. \end{aligned} \tag{15}$$

When applying averaging, we will consider the full system; in our numerical analysis we will consider the cases of $3, 10$ and 20 modes. We note that the normal mode solutions do not satisfy system (14).

If the sequence of eigenvalues is nonresonant, for initial values that are ε-independent and for ε small enough, all solutions will decay to zero; see [10]. The explicit calculation is included in the next subsection.

In general, one can distinguish the following resonance cases:

- Wave speed and dispersion parameter c and ω_0 are $O(1)$ quantities with respect to ε. In this case it is easy to see from the eigenvalue equation (13) that three modes can not be in resonance, but two modes can be in $2:1-$ or $3:1-$resonance. However, because of symmetry, the corresponding normal forms are degenerate; the analysis runs as in [15] where this phenomenon is analyzed extensively.

- The wave speed c is $O(\varepsilon)$. In this case we have, assuming that ω_0 is an $O(1)$ quantity, for a finite number of modes the $1:1:1:\cdots$-resonance. This number depends on ε.

- The dispersion is small: $\omega_0 = O(\varepsilon)$. In this case the system is fully resonant. This problem is unsolved, see for instance the discussion in [16], chapter 13.

3.2 The case of one Floquet resonance

A nontrivial case arises if one of the eigenvalues is close to 1/2, the first Floquet resonance, and there are no other accidental resonances. Suppose that $\omega_m^2 = 0.25 + \varepsilon d$, $m \neq 0$ (as in [10]). Using averaging-normalization in amplitude-phase variables

$$u_n = r_n \cos(\omega_n t + \psi_n),\ \dot{u}_n = -r_n \omega_n \sin(\omega_n t + \psi_n),\ n = 0, 1, 2, \cdots, \tag{16}$$

we find after averaging, with some abuse of notation using the same r_n, ψ_n for the variables,

$$\begin{aligned}
\dot{r}_n &= -\varepsilon \frac{\beta}{2} r_n + O(\varepsilon^2),\ n \neq m, \\
\dot{\psi}_0 &= -\varepsilon \frac{\alpha}{\omega_0} \frac{3}{8} r_0^2 + O(\varepsilon^2),\ \dot{\psi}_n = -\varepsilon \frac{\alpha}{\omega_n} \frac{9}{32} r_n^2 + O(\varepsilon^2),\ n \neq 0, m, \\
\dot{r}_m &= \frac{1}{2} \varepsilon r_m (-\beta + \gamma \sin 2\psi_m) + O(\varepsilon^2), \\
\dot{\psi}_m &= \varepsilon (d + \frac{\gamma}{2} \cos 2\psi_m - \frac{\alpha}{\omega_m} \frac{9}{32} r_m^2) + O(\varepsilon^2)\ (m \neq 0).
\end{aligned}$$

The solution decays to the trivial solution if $\beta > |\gamma|$. Suppose now that $\beta/|\gamma| < 1$ with two solutions for ψ_m from

$$\sin 2\psi_m = \frac{\beta}{\gamma}.$$

Assume $m \neq 0$. Using the two solutions for ψ_m, the equation

$$d + \frac{\gamma}{2} \cos 2\psi_m - \frac{\alpha}{\omega_m} \frac{9}{32} r_m^2 = 0,\ m \neq 0,$$

produces $0, 1$ or 2 solutions for r_m, corresponding (in the case of 1 or 2 solutions) with periodic solutions of the equation for r_m in system (14). The case $m = 0$ runs in the same way.

In the case of one or two solutions, an elementary eigenvalue calculation yields:

$\alpha\gamma \cos 2\psi_m > 0$ produces stability, $\alpha\gamma \cos 2\psi_m < 0$ produces instability.

All the other modes have eigenvalue $-\varepsilon\beta/2$ at $r_n = 0$.

We conclude that the modes with $n \neq m$ decay to zero while the flow in the corresponding Lyapunov manifolds tends to parallel flow. This is the situation described in subsection 2.5: the resonant normal mode m produces a two-dimensional, stable Lyapunov manifold in an ε-neighborhood of the corresponding linear normal mode. The stationary solutions correspond with solutions dominated by harmonic functions.

Note that the approximation theory summarized in subsection 2.2 produces $o(1)$ approximations of the r_n, ψ_n variables for all time when omitting the $O(\varepsilon^2)$ terms in the equations. The Lyapunov manifolds are almost-invariant as discussed in subsection 2.5.

After performing averaging, a large number of numerical simulations were given in [10] for system (14). In many cases the numerics confirms the asymptotic analysis but not always. An interesting case arises when they choose $\alpha = \gamma = 1, \beta = 1/2, \varepsilon = 0.1, d = 0.3$, indicated in [10] as 'point D'. From their simulations they conclude that perturbation theory fails here and this is a reason to have a closer look at this case.

3.3 The combined $1:2$- and $1:1:1$-resonance

Using the parameters of point D and assuming that no other resonance is active, we find one nontrivial critical point in the Lyapunov manifold (normal mode) with m = 1 for $2\psi_m = \pi/6$, a stable focus. Note that if we choose $d > \sqrt{3}/4 = 0.43\ldots$, we have two nontrivial critical points, for $2\psi_m = \pi/6, 5\pi/6$, a stable focus and a saddle. In this case unbounded solutions exist, or formulated more precisely, solutions that leave the domain of validity of the normal form equations. All the other modes should decay. However, this is based on the assumption of having the first Floquet resonance as the only one. Using the parameters of point D, we

find successively

$$\omega_0 = 0.44 + O(\varepsilon), \omega_1 = 0.50 + O(\varepsilon), \omega_2 = 0.66 + O(\varepsilon), \omega_3 = 0.85 + O(\varepsilon), \text{etc.}$$

As in this calculation $\varepsilon = 0.1$, it seems natural to consider this case as a near 1:1:1-resonance. Also, the observation that the ratio $\omega_0 : \omega_3$ points at the presence of an additional $1 : 2$-resonance seems natural, but for the cubic terms of Eq. (12) this resonance is degenerate, i.e normalization shifts the corresponding terms to much higher order.

We have averaged the system truncated to three modes (labeled $0, 1$ and 2) to first and second order. The result is listed in the Appendix. We then performed numerical bifurcation analysis, using MATCONT [8], to see how various modes interact. In the averaged system nontrivial equilibria correspond to periodic solutions in the original system and limit cycles correspond to 2-tori, a Hopf bifurcation of a limit cycle in the averaged system corresponds with a Neimark-Sacker bifurcation in the original system yielding generically a 3-torus. For the bifurcation terminology we refer to [6].

We note that we are interested only in the way the trivial solution becomes unstable, mode solutions appear and interact, but not beyond as this is not captured by the normal form equations. Therefore, in the numerical bifurcation diagram of the averaged equations we show only those bifurcations which occur first when we start with small μ and increase this parameter (we replace ε by $\varepsilon\mu$, put $\varepsilon = 0.1$ and vary μ).

3.3.1 First-order Averaging

From the analysis of the case of one Floquet resonance in section 3.2, it follows that for μ small enough and suitable d, we expect a stable mode 1 periodic solution. Indeed, for $|d| < 0.43\ldots$ the trivial solution is unstable and there are two vertical bifurcation curves, see Fig. 1, where

the origin loses/gains stability upon variation of the parameter d in a pitchfork bifurcation. There are several pitchfork bifurcation curves corresponding to the different modes. At a point where two pitchfork curves intersect, a curve of branch points emanates along which two modes exchange stability. So below the intersection with PF_2^u, a stable mode 1 exists to the right of PF_1^s. Above the intersection, it exists but is unstable between PF_1^s and $BP_{1(1)}$ and is stable to the right of $BP_{1(1)}$.

This solution remains stable except for a region bounded by curve H where this mode solution loses and gains stability in a supercritical Hopf bifurcation when parameters are varied from low to higher d. We note that when restricted to the manifold $u_0 = \dot{u}_0 = u_2 = \dot{u}_2 = 0$, the motion of mode 1 is still stable. In this region, the slightest nonzero perturbation will excite the two other modes and will, in the original vector field, produce dynamics on an invariant torus. Remarkably the point D is just outside this region. Therefore, first order averaging predicts a stable mode 1 solution here, in contradiction with the numerical simulation result in [10]. We stop the discussion of the system obtained by first order averaging by mentioning that there is always a stable mode 2 solution to the right of PF_2^s. Mode 0 exists above PF_0^s and is stable between $BP_{0(1)}$ and $BP_{0(2)}$ and between $BP_{0(3)}$ and $BP_{0(4)}$. First order averaging is generally valid only for $\varepsilon \ll 1$, in the case of our choice of parameters for $\mu < 0.4$.

3.3.2 Second-order Averaging

To check the claim formulated in [10] that perturbation theory has broken down, we use second order averaging to see whether higher order terms will change the result qualitatively. This is probable as the $1:1:1$-resonance acts primarily on the cubic terms at second order normalization. The resulting equations can be found in the Appendix and the results of the bifurcation analysis are shown in Fig. 2. Some bifurcation curves are altered in a

negligible way, primarily those where the trivial solution loses stability and mode solutions appear. For instance, the two vertical pitchfork curves PF_1^u and PF_1^s corresponding to the principal resonance are now slightly bended and the horizontal curve PF_0 is lowered by a small amount. Not so, however, for the stability of the mode 1 solution as the Hopf curve in the higher approximation has altered drastically. Moreover, the region of stability of the mode 1 solution originating from the Floquet resonance, is not only delimited by the curve $BP_{1(1)}$ already present for first-order averaging, but also by $BP_{1(2)}$. Another aspect is that here the curve $BP_{0(1)}$ is connected to $BP_{0(3)}$, and $BP_{0(2)}$ to $BP_{0(4)}$.

If we now consider $d > -.43$ fixed and increase μ, then there are two mechanisms along which the mode 1 solution becomes unstable; We may encounter a branch point or a supercritical Hopf point. The latter occurs for $d > .17$ and $\mu \approx .5$. Increasing μ, the Lyapunov manifold for mode $n = m = 1$ bifurcates upon crossing the lower arc, thus producing a stable periodic solution where the three modes interact. As for the system obtained by first order averaging, the critical point of mode 1 remains stable when restricted to the manifold $u_0 = \dot{u}_0 = u_2 = \dot{u}_2 = 0$. When we further increase μ, this periodic orbit disappears when it has collided with an unstable periodic motion. This scenario follows from the existence of the Generalized Hopf point, where the Hopf bifurcation scenario changes from super- to subcritical. Indeed, Fig. 2 shows the fold of cycles-curve LPC and also another way how the limit cycle may become unstable, i.e. through a supercritical Neimark-Sacker bifurcation. In the original truncated system, this corresponds generically to motion on an invariant three-torus. Finally, the presence of the $R1$-point indicates that this 3-torus will be destructed by touching a homoclinic connection or in a scenario involving periodicity.

3.3.3 Time-T map with 3 modes

To check whether it is sufficient to consider the second order averaging result, we compute the bifurcation diagram of system (14) truncated to the first three modes using the time-T map, with T the period of the forcing. Recall that the frequency of the forcing is twice the internal frequency. This gives a map of which we study the stability of fixed points, using CONTENT [7], and nontrivial fixed points corresponding to periodic orbits in the truncated system. For reasons of comparison we have chosen

$$c^2 = .06 + \varepsilon\mu d, \omega_0^2 = .19, \omega_1^2 = .25 + \varepsilon\mu d, \omega_2^2 = .43 + 4\varepsilon\mu d. \tag{17}$$

The stability boundaries of the trivial solution are now given by several period-doublings PD instead of pitchfork PF curves. The BP curves of Figs. 1 and 2 related to stability exchanges between mode solutions remain branch points. And finally, the Hopf curve turns into a Neimark-Sacker bifurcation and the codimension 2 Generalized Hopf bifurcation into a Chenciner bifurcation. When comparing Figs. 2 and 3, the shape and place of the bifurcation curves is similar except for the curve $BP_{1(2)}$ which is closer to the NS curve for the time-T map than for the second order averaged system. The right analog of PF_2^u does not appear in the time-T map.

Note that algorithms to compute the analogs of the LPC and NS curves of Fig. 2 are unavailable for the time-T map. Instead simulations together with Lyapunov exponents can be used as an indication of the dynamics, see Fig. 4 and Table 1. We focus on the multifrequency scenario. We take $d = 1$ and for $\mu = .4$ we find a fixed point of the second iterate, i.e. a periodic orbit. Increasing μ, we get a motion on a 2-torus as in Fig. 4a. After a further increase the 2-torus doubles near $\mu \approx 0.5428$ and undoubles at $\mu \approx 0.5477$, see Fig. 4b. Then, the 2-torus bifurcates into a stable 3-torus, but it is destroyed quickly in an

μ	λ_1	λ_2	λ_3	λ_4	λ_5	λ_6
0.52	-0.000008	-0.012448	-0.012472	-0.012527	-0.012546	-0.025000
0.5473	0.000009	-0.000692	-0.009205	-0.018167	-0.026665	-0.027374
0.551025	0.000004	0.000002	-0.000018	-0.027534	-0.027552	-0.027555
	0.000009	0.000007	-0.000038	-0.027515	-0.027555	-0.027561
0.56	0.003102	0.000001	-0.004324	-0.023680	-0.027994	-0.031105

Table 1: Lyapunov exponents for attractors shown in Fig. 4.

interaction with another nearby 3-torus. Finally, for a small window of μ, we have chaos, until everything collapses to the trivial solution near $\mu \approx 0.569$. A computation of all Lyapunov exponents, see Table 1, is in agreement with the simulations. Note that we show results for the time-T map, but due to the periodic forcing any nontrivial motion inherits an extra zero exponent in the full system. Note that the doubling is not predicted by averaging and that this occurs for values of μ below the NS-curve in Fig. 2.

3.3.4 Time-T map with 10 modes

It is now clear that the one mode picture does not persist if $\mu \gg .5$. However, it is still of interest whether the three mode picture persists and whether the observed behaviour can be attributed to the 1:1:1 resonance. As a first experiment we consider the first 10 modes and compute the bifurcation curves involving one of the first 3 modes, see Fig. 5. We restricted ourselves to $\mu < 3$ as very large multipliers appeared, making it difficult to extend some computations. Remarkably enough, qualitatively the bifurcation diagram persists for $\mu < 2$. We present the principal bifurcation diagram, although the higher modes bifurcate as well, but play a minor role. We note that mode 1 now also excites all higher order odd modes, but

the amplitude in these modes is very small compared to that of mode 1 ($< 10^{-5}$ for modes 5 – 11 and $< 10^{-12}$ for modes from 13 on). This is in agreement with the estimates in section 2.5.

For higher values of μ, there is an additional Neimark-Sacker bifurcation. Below the curve $BP_{1(2)}$ this multi-frequency motion occurs on a stable submanifold consisting of all the odd modes, i.e. a small perturbation in an even mode decays. Above $BP_{1(2)}$, perturbations quickly distort the multi-frequency oscillation. The end points of this Neimark-Sacker curve are degenerate resonance $1:1$ points, but we have omitted a further analysis of this parameter region as the mode 1 solution is unstable there. We also considered 20 modes with excellent agreement with the results with 10 modes and no extra instabilities for mode 1.

4 Discussion

1. Our explanation for the observations in [10] is, that the small parameter ε and the initial conditions were chosen too large and that the influence of near-resonance was neglected. The latter also explains how the dominant three mode interaction arises from the near $1:1:1$-resonance. Note that perturbation theory has been proved to be valid for ε near zero, but the size of the domain of validity is critically dependent on the type of problem. First order averaging, assuming one Floquet resonance, shows no interaction between the modes and thus one could not predict the interaction with higher modes for larger values of ε. Second order averaging shows strong interaction between the first three modes.

2. From the point of view of numerical bifurcation theory it is interesting that the combination with averaging-normalization is fruitful. The reason is that numerical bifurcation

analysis starts with critical points but that critical points of the averaged vector field already correspond with periodic solutions. So a Hopf bifurcation produces a periodic solution, but in the corresponding map obtained by averaging an invariant closed curve, a 2-torus; a Neimark-Sacker bifurcation of the periodic solution corresponds with a 3-torus etc.

3. We found chaos in the truncated system with three modes in a small window of size 0.001 near $\mu = 0.56$. Simulations indicate that with more than three modes, chaos occurs for slightly larger values of μ and in a larger parameter window. Predictably, second order averaging is not precise enough to describe the phenomenon in this case. Note that in general, averaging-normalization can describe chaos if its measure is large enough.

4. The manifold where the fast dynamics takes place is almost-invariant. We conjecture that the reason that very small fluctuations are possible for the higher order modes arises from the presence of higher order resonance manifolds containing stable and unstable periodic solutions with corresponding intersecting stable and unstable manifolds. These resonance manifolds are of very small size and the analysis to describe them is subtle. For an analysis of such resonance manifolds in two degrees of freedom see [15]. To prove the correctness of the conjecture, more research is needed.

5. The parametrically excited wave equation is also of practical interest; applications are cited in [10]. A number of the phenomena we found, periodic and quasi-periodic solutions, are stable and in this way open for experimental investigation.

5 Appendix

Here we provide details of the first and second order averaging of system (14) expanded into 3 modes.

First of all, in order to consider the 3 mode system as a detuned 1:1:1 resonance, we introduce the following frequencies

$$\Omega_1 = .25 - \varepsilon c_1, \Omega_2 = .25 + \varepsilon\mu d, \Omega_3 = .25 + 3\varepsilon c_1 + 4\varepsilon\mu d.$$

If we fix $\varepsilon = .1, c_1 = .6$, we recover the choice used in [10], but note that this induces a scaling such that $\mu = O(1)$ and c_1 is similar to but not the same as c^2 in (17). We will consider μ and d as free parameters.

Second, we rewrite (14) as a first order system and use the standard transformation

$$\begin{aligned} u_n &= y_{n_1} \cos \omega_n t + \frac{y_{n_2}}{\omega_n} \sin \omega_n t, \\ \dot{u}_n &= -\omega_n y_{n_1} \sin \omega_n t + y_{n_2} \cos \omega_n t, \ n = 0, 1, 2. \end{aligned}$$

Solving for $\frac{dy_{n_1}}{dt}, \frac{dy_{n_2}}{dt}, n = 0, 1, 2$, i.e. the variation of constants, we obtain a system

$$\dot{y} = \varepsilon f(t, y).$$

We calculate the average

$$f^0 = \lim_{T\to\infty} \frac{1}{T} \int_0^T f(t, y)dt = \frac{1}{2\pi} \int_0^{2\pi} f(t, y)dt.$$

The second equality follows from the periodicity of f. For the second order approximation we compute the following integral

$$u^1(t, y) = \int_0^t \left(f(t, y) - f^0\right) dt - \frac{1}{2\pi} \int_0^{2\pi} \left(\int_0^t f(t, y) - f^0 \right) dt,$$

where the second term ensures that the average of u^1 vanishes. Then the higher order approximation by second order averaging is obtained from the average of:

$$f^{10} = D_y f(t, y).u^1 - D_y u^1.f^0,$$

where the second term vanishes as the average of u^1 is zero. The vector field that we now consider is

$$\dot{y} = \varepsilon f^0(y) + \varepsilon^2 f^{10}(y). \tag{18}$$

Note that the validity of this approximation has only been shown for finite dimensional systems with periodic, not almost-periodic, perturbations.

Below we list the result of averaging, i.e. f^0 and $f^{10} = \left(f_1^{10}(y), f_2^{10}(y) \dots \right)^T$, for complete-

ness.

$$f^0(y) = \left(\begin{array}{l} (-2c_1 - \mu)\, y_{0_2} - \frac{1}{4}\mu y_{0_1} - \frac{3}{8}\mu \left(24 y_{0_2} y_{1_2}^2 + 24 y_{0_2} y_{2_2}^2 + 12 y_{1_2}^2 y_{2_2} + 4 y_{0_1} y_{1_1} y_{1_2}\right. \\ \left. +2 y_{0_2} y_{1_1}^2 + 4 y_{0_1}^2 y_{0_2} + y_{1_1}^2 y_{2_2} + 2 y_{0_2} y_{2_1}^2 + 2 y_{1_1} y_{1_2} y_{2_1} + 4 y_{0_1} y_{2_1} y_{2_2} + 16 y_{0_2}^3\right), \\ \frac{1}{4}\left(-\mu + 2c_1\right) y_{0_1} - \frac{1}{4}\mu y_{0_2} + \frac{9}{16}\mu \left(\frac{2}{3} y_{0_1}^3 + \left(y_{1_1}^2 + \frac{8}{3} y_{0_2}^2 + \frac{4}{3} y_{1_2}^2 + \frac{4}{3} y_{2_2}^2\right.\right. \\ \left.\left. +y_{2_1}^2\right) y_{0_1} + \frac{1}{2} y_{1_1}^2 y_{2_1} + \frac{4}{3} y_{1_2}\left(y_{2_2} + 2 y_{0_2}\right) y_{1_1} + \frac{8}{3}\left(\frac{1}{4} y_{1_2}^2 + y_{2_2} y_{0_2}\right) y_{2_1}\right), \\ \mu\left(\left(2d - 4\right) y_{1_2} - \frac{1}{4} y_{1_1}\right) - \frac{9}{8}\left(4 y_{1_2}^3 + \left(16 y_{0_2}^2 + \frac{4}{3} y_{0_1}^2 + \frac{4}{3} y_{2_1} y_{0_1} + y_{1_1}^2 + 8 y_{2_2}^2\right.\right. \\ \left.\left. +\frac{2}{3} y_{2_1}^2 + 16 y_{2_2} y_{0_2}\right) y_{1_2} + \frac{4}{3} y_{1_1}\left(\left(y_{2_1} + 2 y_{0_1}\right) y_{0_2} + y_{2_2}\left(y_{2_1} + y_{0_1}\right)\right)\right) \mu, \\ -\frac{1}{4}\mu\left(y_{1_2} + 2d y_{1_1} + y_{1_1}\right) + \frac{9}{32}\left(y_{1_1}^3 + \left(\frac{16}{3} y_{2_2} y_{0_2} + 2 y_{2_1}^2 + 4 y_{1_2}^2 + \frac{8}{3} y_{2_2}^2\right.\right. \\ \left.\left. +4 y_{2_1} y_{0_1} + \frac{16}{3} y_{0_2}^2 + 4 y_{0_1}^2\right) y_{1_1} + \frac{16}{3} y_{1_2}\left(\left(y_{2_1} + 2 y_{0_1}\right) y_{0_2} + y_{2_2}\left(y_{2_1} + y_{0_1}\right)\right)\right) \mu, \\ \left(\left(-1 + 8d\right)\mu + 6c_1\right) y_{2_2} - \frac{1}{4}\mu y_{2_1} - \frac{3}{4}\mu \left(6 y_{2_2}^3 + \left(12 y_{1_2}^2 + 2 y_{0_1}^2 + y_{1_1}^2 + 24 y_{0_2}^2\right.\right. \\ \left.\left. +\frac{3}{2} y_{2_1}^2\right) y_{2_2} + \left(4 y_{2_1} y_{0_1} + 12 y_{1_2}^2 + y_{1_1}^2\right) y_{0_2} + 2 y_{1_1} y_{1_2}\left(y_{2_1} + y_{0_1}\right)\right), \\ \frac{1}{4}\left(\left(-8d - 1\right)\mu - 6c_1\right) y_{2_1} - \frac{1}{4}\mu y_{2_2} + \frac{9}{16}\left(\frac{1}{2} y_{2_1}^3 + \left(2 y_{0_1}^2 + 2 y_{2_2}^2 + y_{1_1}^2 + \frac{8}{3} y_{0_2}^2\right.\right. \\ \left.\left. +\frac{4}{3} y_{1_2}^2\right) y_{2_1} + y_{0_1} y_{1_1}^2 + \frac{8}{3} y_{1_2}\left(y_{0_2} + y_{2_2}\right) y_{1_1} + \frac{16}{3} y_{0_1}\left(\frac{1}{4} y_{1_2}^2 + y_{2_2} y_{0_2}\right)\right) \mu. \end{array} \right) \tag{19}$$

$$
f_1^{10}(y) = \left(\begin{array}{l}
\frac{1}{256}\left(-13056y_{0_2}^5 + \left(-3264y_{2_1}^2 - 2560 - 6528y_{0_1}^2 - 65280y_{2_2}^2 - 3264y_{1_1}^2 - 65280y_{1_2}^2\right) y_{0_2}^3\right. \\
+\left(-97920y_{1_2}^2 y_{2_2} - 9792y_{1_2}\left(y_{2_1} + 2y_{0_1}\right) y_{1_1} - 4896y_{2_2}\left(4y_{2_1}y_{0_1} + y_{1_1}^2\right)\right) y_{0_2}^2 \\
+\left(-24480y_{1_2}^4 + \left(-7344y_{1_1}^2 - 78336y_{2_2}^2 - 9792y_{0_1}^2 - 9792y_{2_1}y_{0_1} - 3840 + 4608d\right.\right. \\
\left.-4608y_{2_1}^2\right) y_{1_2}^2 - 14976\left(\tfrac{17}{13}y_{0_1} + y_{2_1}\right) y_{2_2}y_{1_2}y_{1_1} - 19584y_{2_2}^4 + \left(18432d - 6048y_{2_1}^2\right. \\
\left.-4608y_{1_1}^2 - 9792y_{0_1}^2 - 3840\right) y_{2_2}^2 - 306y_{1_1}^4 + \left(-2448y_{0_1}^2 - 2448y_{2_1}y_{0_1} - 1152y_{2_1}^2\right. \\
\left.+384d\right) y_{1_1}^2 - 288y_{2_1}^4 + \left(1536d - 2448y_{0_1}^2\right) y_{2_1}^2 - 96 - 816y_{0_1}^4\Big) y_{0_2} - 14688y_{1_2}^4 y_{2_2} \\
-3024\left(\tfrac{34}{21}y_{0_1} + y_{2_1}\right) y_{1_1}y_{1_2}^3 + 6912\left(-\tfrac{119}{48}y_{2_2}^2 - \tfrac{5}{18} - \tfrac{13}{12}y_{2_1}y_{0_1} - \tfrac{17}{24}y_{0_1}^2 - \tfrac{25}{64}y_{2_1}^2\right. \\
\left.+d - \tfrac{5}{8}y_{1_1}^2\right) y_{2_2}y_{1_2}^2 + 1152y_{1_1}\left(\left(-\tfrac{13}{2}y_{0_1} - \tfrac{69}{16}y_{2_1}\right) y_{2_2}^2 + \left(-\tfrac{17}{16}y_{0_1} - \tfrac{21}{32}y_{2_1}\right) y_{1_1}^2\right. \\
-\tfrac{25}{64}y_{2_1}^3 - \tfrac{13}{8}y_{0_1}y_{2_1}^2 + \left(d - \tfrac{17}{8}y_{0_1}^2\right) y_{2_1} + \tfrac{2}{3}\left(d - \tfrac{17}{8}y_{0_1}^2\right) y_{0_1}\Big) y_{1_2} + \left(-900y_{1_1}^2\right. \\
\left.-3744y_{2_1}y_{0_1}\right) y_{2_2}^3 + \left(-162y_{1_1}^4 + \left(-1224y_{0_1}^2 - 1872y_{2_1}y_{0_1} + 576d - 621y_{2_1}^2\right) y_{1_1}^2\right. \\
+3072y_{2_1}\left(-\tfrac{39}{128}y_{2_1}^2 - \tfrac{17}{32}y_{0_1}^2 + d\right) y_{0_1}\Big) y_{2_2} - 64y_{0_1}\Big) \mu^2 + \tfrac{3}{4}\left(-32y_{0_2}^3\right. \\
+\left(48y_{2_2}^2 - 2y_{1_1}^2 - 8y_{0_1}^2 - \tfrac{8}{3} + 4y_{2_1}^2 - 24y_{1_2}^2\right) y_{0_2} + 12y_{1_2}^2 y_{2_2} + 2y_{1_1}\left(-2y_{0_1} + y_{2_1}\right) y_{1_2} \\
\left.+y_{2_2}\left(y_{1_1}^2 + 8y_{2_1}y_{0_1}\right)\right) c_1\mu - 2c_1^2 y_{0_2}
\end{array} \right) \tag{20}
$$

$$
f_2^{10}(y) = \left(\begin{array}{l}
\frac{1}{1024}\left(816y_{0_1}^5 + \left(3264y_{1_2}^2 + 3264y_{2_2}^2 + 4080y_{1_1}^2 + 4080y_{2_1}^2 - 640 + 6528y_{0_2}^2\right)y_{0_1}^3\right. \\
+\left(6120y_{1_1}^2 y_{2_1} + 19584y_{1_2}\left(\frac{1}{2}y_{2_2} + y_{0_2}\right)y_{1_1} + 19584\left(y_{0_2}y_{2_2} + \frac{1}{4}y_{1_2}^2\right)y_{2_1}\right)y_{0_1}^2 \\
+\left(1530y_{1_1}^4 + \left(-960 + 9792y_{0_2}y_{2_2} + 4896y_{2_1}^2 + 4608y_{2_2}^2 + 9792y_{0_2}^2 - 1152d\right.\right. \\
\left.+7344y_{1_2}^2\right)y_{1_1}^2 + 19584y_{1_2}\left(\frac{13}{17}y_{2_2} + y_{0_2}\right)y_{2_1}y_{1_1} + 1224y_{2_1}^4 + \left(-960 + 4608y_{1_2}^2\right. \\
\left.+9792y_{0_2}^2 + 6048y_{2_2}^2 - 4608d\right)y_{2_1}^2 + 4896y_{1_2}^4 + \left(39168y_{0_2}y_{2_2} + 39168y_{0_2}^2\right. \\
\left.-1536d + 18432y_{2_2}^2\right)y_{1_2}^2 + 96 - 6144y_{2_2}^2 d + 4608y_{2_2}^4 + 39168y_{2_2}^2 y_{0_2}^2 \\
\left.+13056y_{0_2}^4\right)y_{0_1} + 918y_{1_1}^4 y_{2_1} + 4896y_{1_2}\left(\frac{21}{34}y_{2_2} + y_{0_2}\right)y_{1_1}^3 \\
+4896y_{2_1}\left(\frac{7}{32}y_{2_1}^2 + \frac{15}{17}y_{1_2}^2 + y_{0_2}^2 - \frac{6}{17}d - \frac{5}{51} + \frac{75}{136}y_{2_2}^2 + \frac{26}{17}y_{0_2}y_{2_2}\right)y_{1_1}^2 \\
+26112\left(\left(\frac{39}{136}y_{0_2} + \frac{207}{1088}y_{2_2}\right)y_{2_1}^2 + \left(\frac{63}{136}y_{2_2} + \frac{3}{4}y_{0_2}\right)y_{1_2}^2 + y_{0_2}^3 + \frac{3}{2}y_{0_2}^2 y_{2_2}\right. \\
\left.+\left(\frac{39}{34}y_{2_2}^2 - \frac{2}{17}d\right)y_{0_2} - \frac{3}{17}y_{2_2}\left(-\frac{25}{16}y_{2_2}^2 + d\right)\right)y_{1_2}y_{1_1} + \left(3744y_{0_2}y_{2_2}\right. \\
\left.+900y_{1_2}^2\right)y_{2_1}^3 + \left(2592y_{1_2}^4 + \left(-2304d + 9936y_{2_2}^2 + 29952y_{0_2}y_{2_2} + 19584y_{0_2}^2\right)y_{1_2}^2\right. \\
\left.+26112y_{2_2}y_{0_2}\left(\frac{39}{68}y_{2_2}^2 - \frac{8}{17}d + y_{0_2}^2\right)\right)y_{2_1} + 256y_{0_2}\Big)\mu^2 \\
+6\left(\frac{1}{4}y_{0_1}^3 + \left(-\frac{1}{2}y_{2_2}^2 + y_{0_2}^2 - \frac{3}{8}y_{2_1}^2 - \frac{1}{12} + \frac{3}{16}y_{1_1}^2 + \frac{1}{4}y_{1_2}^2\right)y_{0_1} - \frac{3}{32}y_{1_1}^2 y_{2_1}\right. \\
\left.+\frac{1}{2}y_{1_2}\left(-\frac{1}{2}y_{2_2} + y_{0_2}\right)y_{1_1} - y_{2_1}\left(\frac{1}{8}y_{1_2}^2 + y_{0_2}y_{2_2}\right)\right)c_1\mu + \frac{1}{2}c_1^2 y_{0_1}
\end{array} \right) \tag{21}
$$

$$
f_3^{10}(y) = \left(\begin{array}{l}
-255\left(\left(\frac{9}{80}y_{1_2}^5+\left(\frac{3}{4}y_{2_2}^2-\frac{6}{85}d+\frac{3}{40}y_{0_1}^2+\frac{3}{80}y_{2_1}^2+\frac{3}{2}y_{0_2}^2+\frac{1}{34}+\frac{9}{160}y_{1_1}^2+\frac{9}{5}y_{0_2}y_{2_2}\right.\right.\right. \\
\left.\left.\left.+\frac{27}{340}y_{2_1}y_{0_1}\right)y_{1_2}^3+\frac{189}{680}y_{1_1}\left(\left(\frac{34}{21}y_{0_1}+y_{2_1}\right)y_{0_2}+\frac{17}{21}y_{2_2}\left(y_{2_1}+\frac{21}{17}y_{0_1}\right)\right)y_{1_2}^2\right. \\
+\left(\frac{9}{1280}y_{1_1}^4+\left(\frac{9}{136}y_{2_1}y_{0_1}+\frac{9}{40}y_{0_2}^2+\frac{9}{34}y_{0_2}y_{2_2}+\frac{9}{160}y_{0_1}^2+\frac{9}{80}y_{2_2}^2+\frac{9}{320}y_{2_1}^2\right.\right. \\
\left.\left.-\frac{3}{170}d\right)y_{1_1}^2+y_{0_2}^4+2y_{2_2}y_{0_2}^3+\left(-\frac{12}{85}d+\frac{12}{5}y_{2_2}^2+\frac{3}{10}y_{2_1}y_{0_1}+\frac{12}{85}y_{2_1}^2+\frac{3}{10}y_{0_1}^2\right. \\
\left.+\frac{2}{17}\right)y_{0_2}^2-\frac{36}{85}\left(-\frac{119}{48}y_{2_2}^2-\frac{25}{64}y_{2_1}^2-\frac{13}{12}y_{2_1}y_{0_1}-\frac{5}{18}+d-\frac{17}{24}y_{0_1}^2\right)y_{2_2}y_{0_2} \\
+\frac{3}{10}y_{2_2}^4+\left(\frac{12}{85}y_{0_1}^2+\frac{63}{680}y_{2_1}^2+\frac{1}{17}+\frac{207}{1360}y_{2_1}y_{0_1}-\frac{6}{17}d\right)y_{2_2}^2+\frac{3}{680}y_{2_1}^4+ \\
\frac{15}{1088}y_{2_1}^3y_{0_1}+\left(\frac{3}{85}y_{0_1}^2-\frac{1}{34}d\right)y_{2_1}^2+\left(-\frac{3}{85}y_{0_1}d+\frac{1}{4}0y_{0_1}^3\right)y_{2_1}+\frac{2}{255}d^2 \\
\left.+\frac{1}{80}y_{0_1}^4+\frac{1}{680}-\frac{1}{85}y_{0_1}^2d-\frac{2}{255}d\right)y_{1_2}+\frac{1}{10}y_{1_1}\left(\left(\left(\frac{3}{8}y_{0_1}+\frac{63}{272}y_{2_1}\right)y_{0_2}\right.\right. \\
\left.\left.+\frac{3}{16}y_{2_2}\left(y_{2_1}+\frac{21}{17}y_{0_1}\right)\right)y_{1_1}^2+\left(y_{2_1}+2y_{0_1}\right)y_{0_2}^3+\frac{39}{17}\left(\frac{17}{13}y_{0_1}+y_{2_1}\right)y_{2_2}y_{0_2}^2+\right. \\
\left(\left(\frac{207}{136}y_{2_1}+\frac{39}{17}y_{0_1}\right)y_{2_2}^2+\frac{75}{544}y_{2_1}^3+\frac{39}{68}y_{0_1}y_{2_1}^2+\left(-\frac{6}{17}d+\frac{3}{4}y_{0_1}^2\right)y_{2_1}-\frac{4}{17}y_{0_1}d\right. \\
\left.+\frac{1}{2}y_{0_1}^3\right)y_{0_2}+\frac{1}{102}+\left(\frac{75}{136}y_{0_1}+\frac{39}{68}y_{2_1}\right)y_{2_2}^3+\left(\frac{39}{272}y_{2_1}^3+\frac{207}{544}y_{0_1}y_{2_1}^2\right. \\
\left.+\left(\frac{39}{68}y_{0_1}^2-\frac{10}{17}d\right)y_{2_1}-\frac{6}{17}y_{0_1}d+\frac{1}{4}y_{0_1}^3\right)y_{2_2}\Big)\mu \\
+\frac{12}{85}c_1\left(\left(-y_{0_2}y_{2_2}+\frac{1}{12}y_{0_1}^2+y_{0_2}^2-\frac{3}{2}y_{2_2}^2-\frac{1}{12}y_{2_1}y_{0_1}-\frac{1}{8}y_{2_1}^2\right)y_{1_2}\right. \\
\left.\left.-\frac{1}{12}y_{1_1}\left(\left(-2y_{0_1}+y_{2_1}\right)y_{0_2}+3y_{2_2}\left(\frac{1}{3}y_{0_1}+y_{2_1}\right)\right)\right)\mu
\end{array} \right) \tag{22}
$$

$$
f_4^{10}(y) = \left(\begin{array}{l}
\frac{51}{4}\mu \left(\left(\frac{9}{256} y_{1_1}^5 + \left(\frac{9}{16} y_{2_1} y_{0_1} + \frac{9}{32} y_{1_2}^2 + \frac{15}{32} y_{0_1}^2 + \frac{15}{64} y_{2_1}^2 + \frac{3}{8} y_{0_2}^2 - \frac{3}{34} d + \frac{3}{16} y_{2_2}^2 \right.\right.\right. \\
\left. + \frac{27}{68} y_{0_2} y_{2_2} - \frac{5}{136} \right) y_{1_1}^3 + \frac{189}{136} y_{1_2} \left(\left(y_{0_2} + \frac{17}{21} y_{2_2} \right) y_{2_1} + \frac{34}{21} y_{0_1} \left(y_{0_2} + \frac{21}{34} y_{2_2} \right) \right) y_{1_1}^2 \\
+ \left(\frac{9}{16} y_{1_2}^4 + \left(\frac{9}{4} y_{2_2}^2 + \frac{9}{2} y_{0_2}^2 + \frac{9}{16} y_{2_1}^2 + \frac{90}{17} y_{0_2} y_{2_2} + \frac{45}{34} y_{2_1} y_{0_1} + \frac{9}{8} y_{0_1}^2 - \frac{6}{17} d \right) y_{1_2}^2 \right. \\
+ \frac{3}{32} y_{2_1}^4 + \frac{21}{64} y_{2_1}^3 y_{0_1} + \left(\frac{63}{136} y_{2_2}^2 - \frac{15}{34} d + \frac{3}{4} y_{0_1}^2 + \frac{12}{17} y_{0_2}^2 + \frac{207}{272} y_{0_2} y_{2_2} - \frac{5}{68} \right) y_{2_1}^2 \\
+ \frac{3}{2} y_{0_1} \left(\frac{5}{12} y_{0_1}^2 + \frac{26}{17} y_{0_2} y_{2_2} - \frac{6}{17} d + y_{0_2}^2 + \frac{75}{136} y_{2_2}^2 - \frac{5}{51} \right) y_{2_1} + \frac{5}{16} y_{0_1}^4 + \\
\left(-\frac{5}{34} + \frac{3}{2} y_{0_2} y_{2_2} + \frac{3}{2} y_{0_2}^2 - \frac{3}{17} d + \frac{12}{17} y_{2_2}^2 \right) y_{0_1}^2 + y_{0_2}^4 + 2 y_{2_2} y_{0_2}^3 + \left(-\frac{4}{17} d + \frac{48}{17} y_{2_2}^2 \right) y_{0_2}^2 \\
\left. + \left(-\frac{12}{17} y_{2_2} d + \frac{75}{68} y_{2_2}^3 \right) y_{0_2} - \frac{10}{17} y_{2_2}^2 d + \frac{2}{51} d^2 + \frac{2}{51} d + \frac{6}{17} y_{2_2}^4 + \frac{1}{136} \right) y_{1_1} \\
+ 2 y_{1_2} \left(\left(\left(\frac{63}{68} y_{0_2} + \frac{3}{4} y_{2_2} \right) y_{2_1} + \frac{3}{2} y_{0_1} \left(y_{0_2} + \frac{21}{34} y_{2_2} \right) \right) y_{1_2}^2 + \left(\frac{75}{544} y_{0_2} + \frac{39}{272} y_{2_2} \right) y_{2_1}^3 \right. \\
+ \frac{39}{68} \left(\frac{69}{104} y_{2_2} + y_{0_2} \right) y_{0_1} y_{2_1}^2 + \left(\left(\frac{3}{4} y_{0_2} + \frac{39}{68} y_{2_2} \right) y_{0_1}^2 + y_{0_2}^3 + \frac{39}{17} y_{0_2}^2 y_{2_2} \right. \\
+ \left(\frac{207}{136} y_{2_2}^2 - \frac{6}{17} d \right) y_{0_2} - \frac{10}{17} y_{2_2} d + \frac{39}{68} y_{2_2}^3 \Big) y_{2_1} + \frac{1}{102} + \left(\frac{1}{4} y_{2_2} + \frac{1}{2} y_{0_2} \right) y_{0_1}^3 \\
\left. \left. + \left(2 y_{0_2}^3 + 3 y_{0_2}^2 y_{2_2} + \left(\frac{39}{17} y_{2_2}^2 - \frac{4}{17} d \right) y_{0_2} + \frac{75}{136} y_{2_2}^3 - \frac{6}{17} y_{2_2} d \right) y_{0_1} \right) \right) \mu \\
+ \frac{4}{17} c_1 \left(\left(\frac{3}{4} y_{0_1}^2 - y_{0_2} y_{2_2} + y_{0_2}^2 - \frac{3}{4} y_{2_1} y_{0_1} - \frac{3}{2} y_{2_2}^2 - \frac{9}{8} y_{2_1}^2 \right) y_{1_1} \right. \\
\left. \left. - \left(\left(3 y_{2_2} + y_{0_2} \right) y_{2_1} - 2 \left(-\frac{1}{2} y_{2_2} + y_{0_2} \right) y_{0_1} \right) y_{1_2} \right)
\end{array} \right) \tag{23}
$$

$$
f_5^{10}(y) = \left(\begin{array}{l}
\frac{1}{256}\left(-7344y_{2_2}^5 + \left(-3672y_{2_1}^2 - 2304y_{1_1}^2 - 4608y_{0_1}^2 - 78336y_{0_2}^2 - 1920 - 39168y_{1_2}^2\right.\right. \\
\left.\left.+18432d\right)y_{2_2}^3 + \left(-102816y_{0_2}y_{1_2}^2 - 11232\left(\frac{25}{26}y_{0_1} + y_{2_1}\right)y_{1_1}y_{1_2}\right.\right. \\
\left.\left. + \left(-5400y_{1_1}^2 - 22464y_{2_1}y_{0_1}\right)y_{0_2}\right)y_{2_2}^2 + \left(-24480y_{1_2}^4 + \left(-156672y_{0_2}^2 - 7344y_{1_1}^2\right.\right.\right. \\
\left.\left.\left.-9216y_{0_1}^2 - 3840 + 23040d - 6048y_{2_1}^2 - 9936y_{2_1}y_{0_1}\right)y_{1_2}^2 - 65280y_{0_2}^4\right. \\
-19872y_{0_2}y_{1_1}\left(y_{2_1} + \frac{104}{69}y_{0_1}\right)y_{1_2} + \left(-12096y_{2_1}^2 - 19584y_{0_1}^2 - 9216y_{1_1}^2 - 7680\right. \\
\left.+36864d\right)y_{0_2}^2 - 306y_{1_1}^4 + \left(-1512y_{2_1}^2 + 1920d - 2304y_{0_1}^2 - 2700y_{2_1}y_{0_1}\right)y_{1_1}^2 \\
-459y_{2_1}^4 + \left(-3024y_{0_1}^2 + 4608d\right)y_{2_1}^2 - 96 + 2048d - 816y_{0_1}^4 + 3072dy_{0_1}^2 \\
\left.-8192d^2\right)y_{2_2} - 29376y_{1_2}^4y_{0_2} - 4896y_{1_1}\left(y_{2_1} + \frac{21}{17}y_{0_1}\right)y_{1_2}^3 - 65280y_{0_2}\left(\frac{39}{170}y_{2_1}y_{0_1}\right. \\
\left.+y_{0_2}^2 + \frac{1}{17} + \frac{45}{544}y_{2_1}^2 - \frac{18}{85}d + \frac{9}{68}y_{1_1}^2 + \frac{3}{20}y_{0_1}^2\right)y_{1_2}^2 - 14976\left(\left(\frac{17}{13}y_{0_1} + y_{2_1}\right)y_{0_2}^2 + \right. \\
\left.\left(\frac{21}{208}y_{0_1} + \frac{17}{208}y_{2_1}\right)y_{1_1}^2 + \frac{1}{16}y_{2_1}^3 + \frac{69}{416}y_{0_1}y_{2_1}^2 + \left(-\frac{10}{39}d + \frac{1}{4}y_{0_1}^2\right)y_{2_1}\right. \\
\left.-\frac{2}{13}y_{0_1}\left(-\frac{17}{24}y_{0_1}^2 + d\right)\right)y_{1_1}y_{1_2} + \left(-13056y_{2_1}y_{0_1} - 3264y_{1_1}^2\right)y_{0_2}^3 + \left(-324y_{1_1}^4 + \right. \\
\left.\left(-1242y_{2_1}^2 - 2448y_{0_1}^2 + 1152d - 3744y_{2_1}y_{0_1}\right)y_{1_1}^2 - 1872y_{2_1}y_{0_1}\left(\frac{68}{39}y_{0_1}^2 + y_{2_1}^2\right.\right. \\
\left.\left.\left.-\frac{128}{39}d\right)\right)y_{0_2} - 64y_{2_1}\right)\mu^2 + 72\left(\frac{3}{4}y_{2_2}^3 + \left(-\frac{2}{3}d + \frac{3}{4}y_{1_2}^2 + \frac{1}{12}y_{0_1}^2 + \frac{3}{16}y_{2_1}^2 + \frac{1}{16}y_{1_1}^2\right.\right. \\
\left.\left.+\frac{1}{12} + y_{0_2}^2\right)y_{2_2} + \frac{1}{4}y_{0_2}y_{1_2}^2 + \frac{1}{8}y_{1_1}\left(\frac{1}{3}y_{0_1} + y_{2_1}\right)y_{1_2} + \frac{1}{4}8y_{0_2}\left(y_{1_1}^2 + 8y_{2_1}y_{0_1}\right)\right)c_1\mu \\
-18c_1^2y_{2_2}
\end{array} \right) \tag{24}
$$

$$
f_6^{10}(y) = \left(\begin{array}{l}
\frac{1}{1024}\left(459y_{2_1}^5 + \left(4608y_{0_2}^2 + 4896y_{0_1}^2 - 4608d + 3672y_{2_2}^2 + 2304y_{1_2}^2 + 2448y_{1_1}^2\right.\right. \\
\left.-480\right)y_{2_1}^3 + \left(6426y_{1_1}^2 y_{0_1} + 11232\left(y_{2_2} + \frac{25}{26}y_{0_2}\right)y_{1_2}y_{1_1} + (22464y_{2_2}y_{0_2}\right. \\
\left.+5400y_{1_2}^2\right)y_{0_1}\Big)y_{2_1}^2 + \left(1530y_{1_1}^4 + \left(9792y_{0_1}^2 + 9216y_{0_2}^2 - 960 + 7344y_{1_2}^2\right.\right. \\
\left.+9936y_{2_2}y_{0_2} - 5760d + 6048y_{2_2}^2\right)y_{1_1}^2 + 19872y_{1_2}\left(\frac{104}{69}y_{0_2} + y_{2_2}\right)y_{0_1}y_{1_1} + 4080y_{0_1}^4 + \\
\left(12096y_{2_2}^2 - 1920 + 9216y_{1_2}^2 - 9216d + 19584y_{0_2}^2\right)y_{0_1}^2 + 4896y_{1_2}^4 + \\
\left(-7680d + 36864y_{0_2}^2 + 43200y_{2_2}y_{0_2} + 24192y_{2_2}^2\right)y_{1_2}^2 + 7344y_{2_2}^4 + \\
\left(-18432d + 48384y_{0_2}^2\right)y_{2_2}^2 + 96 - 12288dy_{0_2}^2 + 2048d + 8192d^2 + 13056y_{0_2}^4\Big)y_{2_1} \\
+1836y_{1_1}^4 y_{0_1} + 4896\left(y_{2_2} + \frac{21}{17}y_{0_2}\right)y_{1_2}y_{1_1}^3 + 5400\left(\frac{34}{45}y_{0_1}^2 + y_{2_2}^2 + \frac{136}{75}y_{0_2}^2\right. \\
\left.+\frac{208}{75}y_{2_2}y_{0_2} - \frac{8}{45} + \frac{8}{5}y_{1_2}^2 - \frac{16}{25}d\right)y_{0_1}y_{1_1}^2 + 14976y_{1_2}\left(\left(y_{2_2} + \frac{17}{13}y_{0_2}\right)y_{0_1}^2 + \right. \\
\left.\left(\frac{17}{13}y_{2_2} + \frac{21}{13}y_{0_2}\right)y_{1_2}^2 + y_{2_2}^3 + \frac{69}{26}y_{0_2}y_{2_2}^2 + \left(-\frac{40}{39}d + 4y_{0_2}^2\right)y_{2_2} - \frac{8}{13}y_{0_2}d + \frac{68}{39}y_{0_2}^3\right)y_{1_1} \\
+\left(3264y_{1_2}^2 + 13056y_{2_2}y_{0_2}\right)y_{0_1}^3 + \left(5184y_{1_2}^4 + \left(19872y_{2_2}^2 - 4608d + 39168y_{0_2}^2\right.\right. \\
\left.\left.+59904y_{2_2}y_{0_2}\right)y_{1_2}^2 + 29952\left(-\frac{32}{39}d + y_{2_2}^2 + \frac{68}{39}y_{0_2}^2\right)y_{0_2}y_{2_2}\right)y_{0_1} + 256y_{2_2}\Big)\mu^2 \\
-\frac{27}{2}\left(\frac{1}{4}y_{2_1}^3 + \left(\frac{1}{4}y_{1_1}^2 + y_{2_2}^2 + \frac{1}{3}y_{0_1}^2 + \frac{4}{9}y_{0_2}^2 - \frac{1}{9} + \frac{1}{3}y_{1_2}^2 - \frac{8}{9}d\right)y_{2_1} + \frac{1}{12}y_{1_1}^2 y_{0_1}\right. \\
\left.+\frac{2}{3}y_{1_2}\left(y_{2_2} + \frac{1}{3}y_{0_2}\right)y_{1_1} + \frac{8}{9}\left(\frac{1}{8}y_{1_2}^2 + y_{2_2}y_{0_2}\right)y_{0_1}\right)c_1\mu + \frac{9}{2}c_1^2 y_{2_1}
\end{array} \right) \tag{25}
$$

Acknowledgment

Peter Bates and Stephan van Gils made remarks on an early draft of the paper. Remarks and questions by two anonymous referees have resulted in substantial changes.

References

[1] P.W. Bates and C.K.R.T. Jones, *Invariant manifolds for semilinear partial differential equations*, Dynamics Reported 2, (1989) pp. 1-38.

[2] P.W. Bates, K. Lu and C. Zeng, *Existence and persistence of invariant manifolds for semiflows in Banach space*, Mem. Amer. Math. Soc. 135, (1998) no. 645.

[3] P.W. Bates, K. Lu and C. Zeng, *Persistence of overflowing manifolds for semiflow*, Comm. Pure Appl. Math. 12, (1999) pp. 983-1046.

[4] R.P. Buitelaar, *The method of averaging in Banach spaces*, Thesis (1993), University of Utrecht.

[5] D.A. Jones and E.S. Titi, C^1 *Approximations of inertial manifolds for dissipative nonlinear equations*, J. Diff. Equations 127, (1996) pp. 54-86.

[6] Yu.A. Kuznetsov, *Elements of applied bifurcation theory*, 3d ed., Springer (2004).

[7] Yu.A. Kuznetsov and V.V. Levitin, CONTENT: *A multiplatform environment for analyzing dynamical systems*. (`ftp.cwi.nl/pub/CONTENT`), 1995–2001.

[8] A. Dhooge, W. Govaerts, Yu.A. Kuznetsov, H.G.E. Meijer and B. Sautois, *New features of the software* MATCONT *for bifurcation analysis of dynamical systems.*Math. Comp. Mod. Dyn. Sys., 147–175 (2008).

[9] G. Menon and G. Haller, *Infinite dimensional geometric singular perturbation theory for the Maxwell-Bloch equations*, SIAM J. Math. Anal. 33, (2001) pp. 315-346.

[10] R.H. Rand, W.I. Newman, B.C. Denardo and A.L. Newman, *Dynamics of a nonlinear parametrically-excited partial differential equation*, Proc. 1995 Design Eng. Techn. Conferences 3 (1995) pp. 57-68, ASME, DE-84-1. (See also Newman, Rand and Newman, Chaos 9, pp. 242-253, 1999.)

[11] Jan A. Sanders, Ferdinand Verhulst and James Murdock, *Averaging methods in nonlinear dynamical systems, 2d ed.*, Applied Math. Sciences 59, Springer (2007).

[12] E. Sanchez-Palencia, *Méthode de centrage et comportement des trajectoires dans l'espace des phases*, Ser. A Compt. Rend. Acad. Sci. 280, pp. 105-107, (1975).

[13] E. Sanchez-Palencia, *Méthode de centrage - estimation de l'erreur et comportement des trajectoires dans l'espace des phases*, Int. J. Non-Linear Mechanics 11, pp. 251-263, (1976).

[14] A.P. Seyranian and A.P. Mailybaev, *Multiparameter stability theory with mechanical applications*, World Scientific (2003).

[15] J.M. Tuwankotta and F. Verhulst, *Symmetry and resonance in Hamiltonian systems*, SIAM J. Appl. Math. 61, pp. 1369-1385, (2000).

[16] F. Verhulst, *Methods and applications of singular perturbations, boundary layers and multiple timescale dynamics*, Springer (2005) 340 pp. For comments and corrections, see the website www.math.uu.nl/people/verhulst

[17] R.W. Wittenberg and P. Holmes, *The limited effectiveness of normal forms: a critical review and extension of local bifurcation studies of the Brusselator PDE*, Physica D 100, pp. 1-40, (1997).

[18] C. Zeng, *Persistence of invariant manifolds of semiflows with symmetry*, Electronic J. Diff. Eqs vol. 1998, (1998) pp. 1-13.

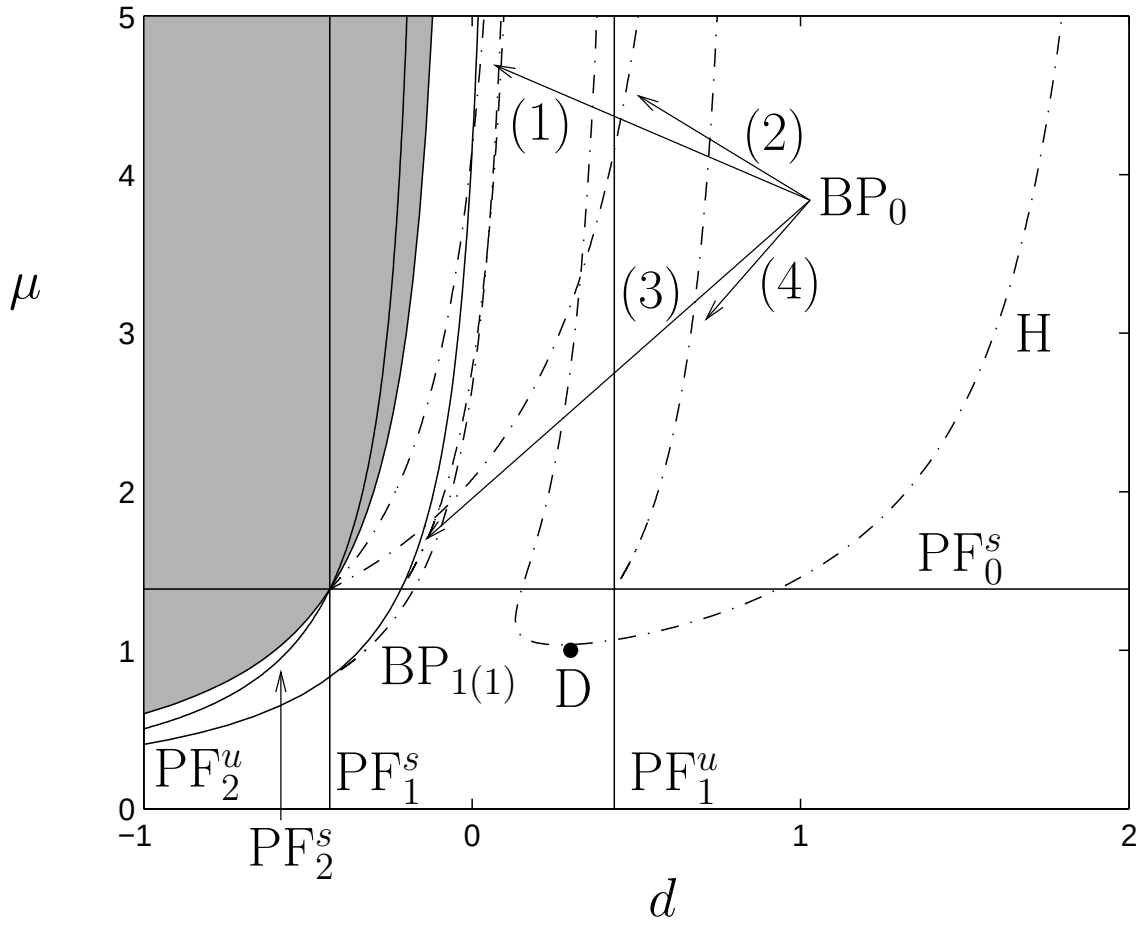

Figure 1: Numerical bifurcation diagram based on first order averaging of system (13) with the assumption of near $1:1:1$-resonance leading to the averaged system (19). Horizontally we have the detuning d, vertically the parameter μ. Labels denote $\mathrm{PF}_i^{u,s}$ = Pitchfork (full lines); $i = 0, 1, 2$ denotes the mode involved, s or u indicates the (in-)stability of the bifurcating critical point. BP_i = Branch Point (dot-dashed); $i = 0, 1, 2$ denotes the mode involved. H = Hopf bifurcation (dot-dashed). The shaded region is unphysical, i.e. $\varepsilon\mu d < -0.06$. The critical point in mode 1 loses stability through the Hopf bifurcation of the averaged equation corresponding to a periodic solution in the Lyapunov manifold of mode 1 in the original system.

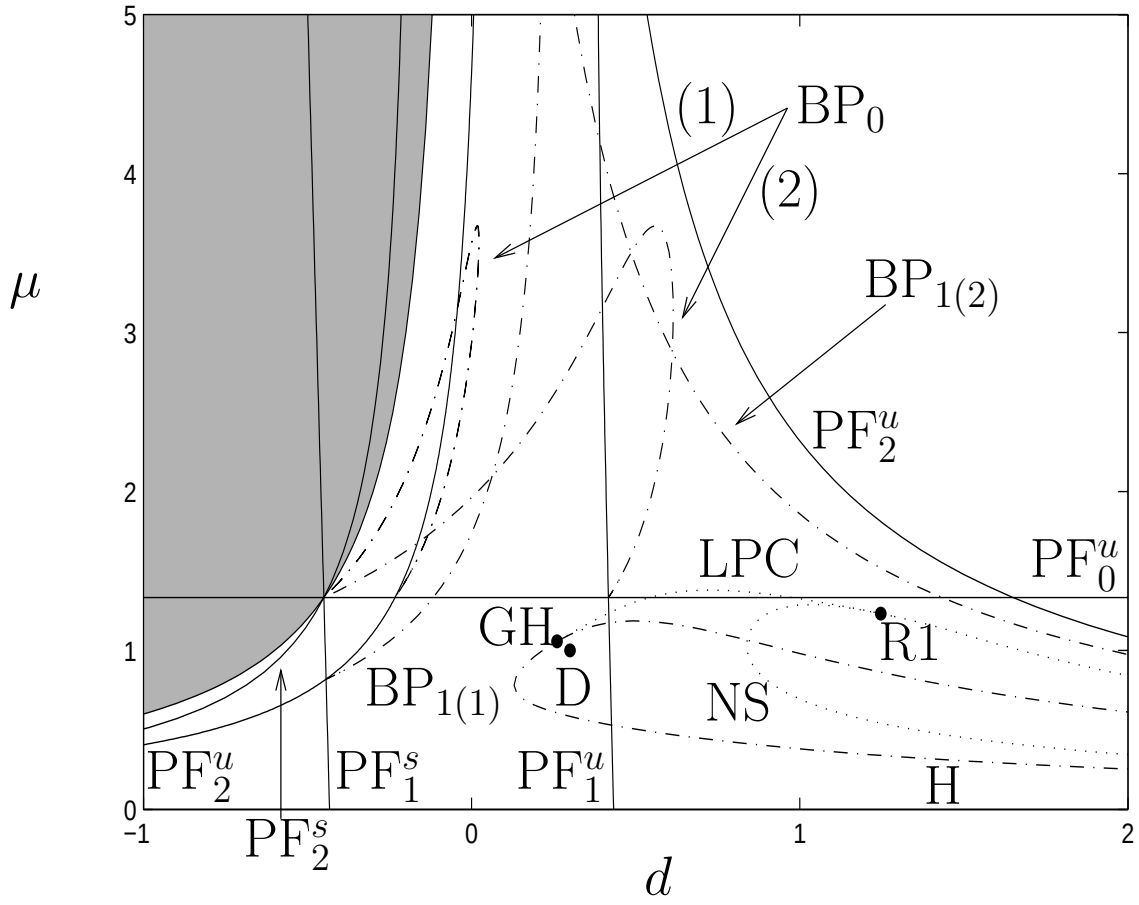

Figure 2: Numerical bifurcation diagram based on second order averaging of system (13) with the assumption of near 1 : 1 : 1-resonance leading to the averaged system (18). Horizontally we have the detuning d, vertically the parameter μ. Labels are analogous as in Fig. 1, except for GH = Generalized Hopf point, LPC = Limit Point of Cycles (dotted), NS = Neimark-Sacker of cycles(dotted) and R1 = Resonance 1:1 point. The curve indicated with H represents the Hopf bifurcation of the critical point of the averaged equation and so to the Neimark-Sacker bifurcation of the corresponding periodic solution in the Lyapunov manifold of mode 1.

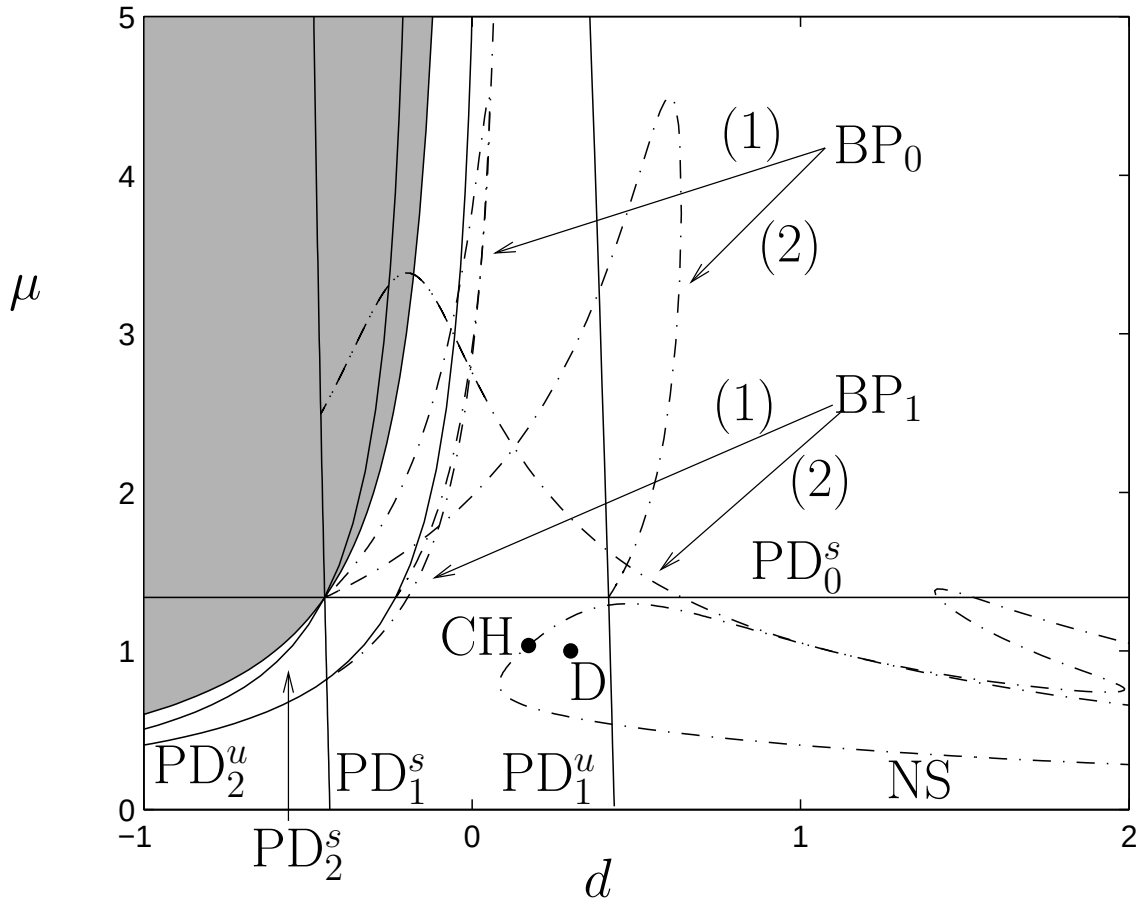

Figure 3: Numerical bifurcation diagram for the first three modes. $\mathrm{PD}_i^{u,s}$ = period-doubling bifurcation of the origin; $i = 0, 1, 2$ denotes the mode involved in the period-doubling and s or u denotes whether the period-2 solution is stable or not. NS = Neimark-Sacker bifurcation, BP_i = Branch Point; $i = 0, 1$ denotes the mode involved. CH = Chenciner point. The point D from [10] is located within the Neimark-Sacker curve (see the main text). On the lower arc the Neimark-Sacker bifurcation is supercritical, while the upper-arc is subcritical and the square (CH) denotes the transition, a Chenciner bifurcation. The shaded area corresponds to $c^2 < 0$.

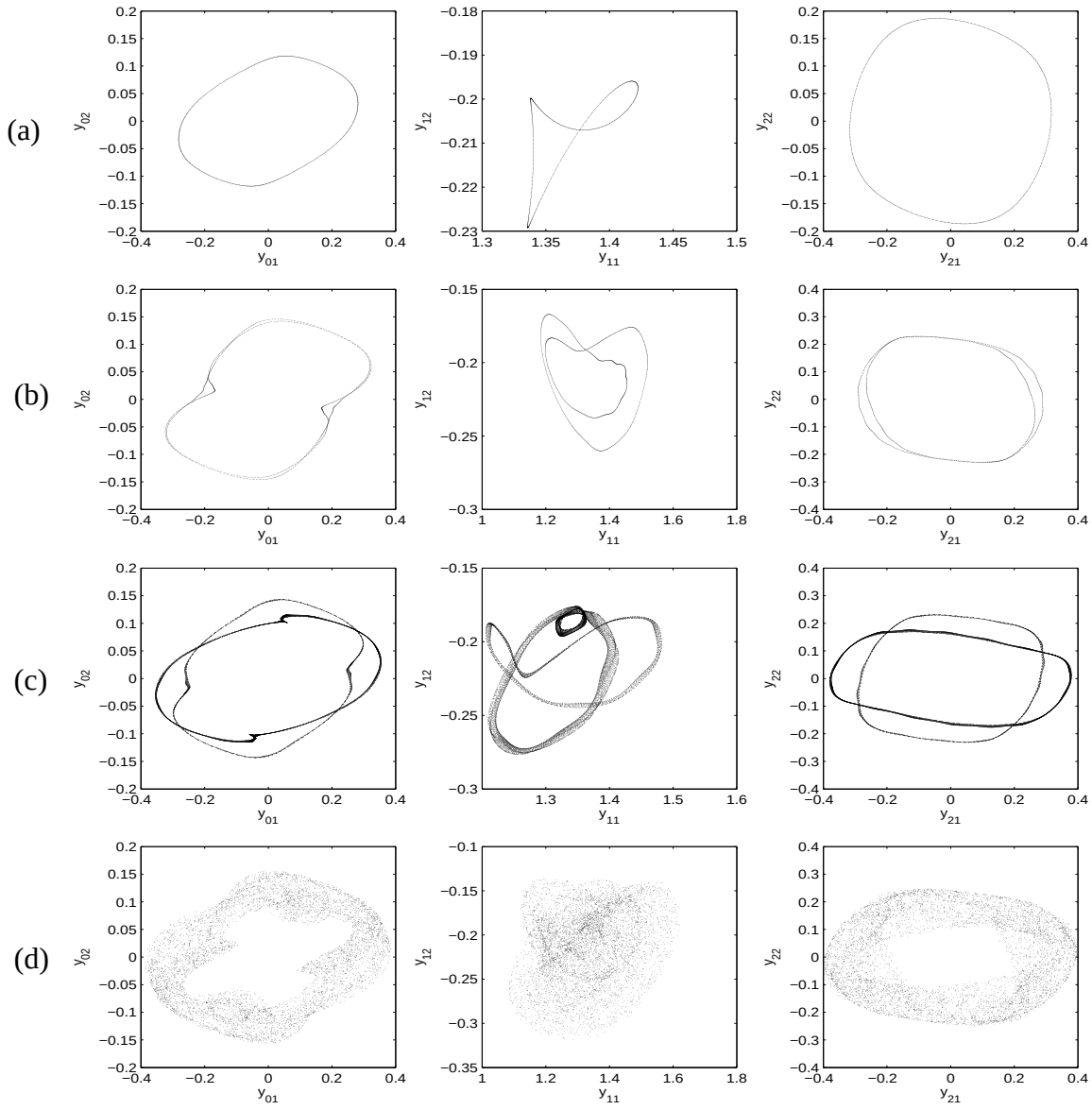

Figure 4: Simulations of the second iterate of time-T map for 3 modes projected onto (y_{0_1}, y_{0_2}), (y_{1_1}, y_{1_2}) and (y_{2_1}, y_{2_2}) planes. (a) $\mu = 0.52$ a torus, (b) $\mu = 0.5473$ a doubled torus, (c) $\mu = 0.551025$ two 3-tori, (d) $\mu = 0.56$ chaos in a small window till $\mu = 0.569$.

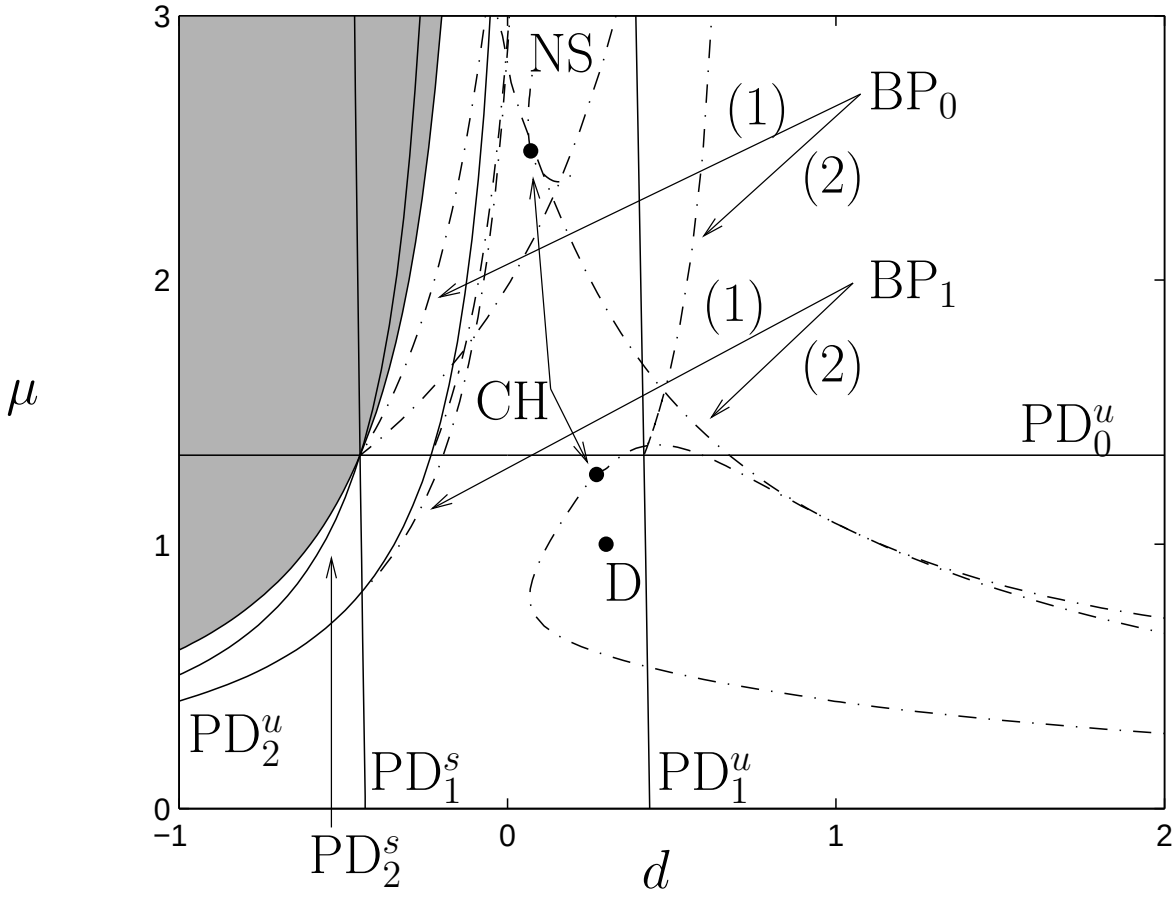

Figure 5: Partial bifurcation diagram for truncation to 10 modes. For μ small enough, the three mode picture persists in the system truncated to 10 modes. The labels are analogous to those of the Fig. 3. Apart from minor dissimilarities there is one extra Neimark-Sacker bifurcation curve for $\mu \approx 2.4$ of which the lower arc is supercritical and the upper subcritical, and another Chenciner bifurcation in between.